

Abstract

This study presents crack initiation, propagation and coalescence at or near pre-existing open cracks in a numerical model under Brazilian test. Firstly, Particle Flow Code in two dimensions (PFC2d) was calibrated with respect to the data obtained from experimental laboratory tests to ensure the conformity of the simulated numerical models response. Brazilian discs contain one, two, three, four, and five parallel centred cracks (45° to the horizontal) under compressive line loading. Models containing two and three cracks have different joint spacing and joint configuration. In model consisting one flaws, tensile cracks initiated from notch tip and propagates in direction of compressive loading till coalesce with model edge. By increasing the number of notch, first type of tensile crack initiated at the tips of outer flaws and coalesced with model edge. Also second type of tensile cracks initiates from middle of inner flaws and coalesce with tip of the neighbouring flaws. The results show that joint spacing and joint configuration has important effect on the failure pattern in model consisting two and three notch. Experimental and numerical results rendered by other researchers showed a good agreement with the numerical results in the coalescence characteristics in cracked model. In addition, crack initiation and coalescence stresses in models were analyzed and compared with those in the single-flawed model.

Keywords

PFC2D, brazilian discs, multiple parallel cracks

1 Introduction

Rock is heterogeneous solids containing cracks. Under different stresses, cracks initiate from defects and coalesce with neighbouring cracks. This process leads to degradation of the strength of solids. Brittle failure of solids containing multiple cracks is one of the most important areas of research in the field of rock mechanics. Extensive research has been performed on the brittle behaviour of jointed rock under compression. In particular, with relevance to this current work, experimental studies have previously been conducted on both “rock-like” materials (Reyes and Einstein 1991; Shen and Stephansson 1993; Shen et al. 1995; Bobet and Einsein 1998; Wong and Chau, 1998; Scavia and Castelli 1998; Mughieda and Alzoubi 2004) and real rock specimens (Ingraffea and Heuze 1980; Petit and Barquins, 1988; Jiefan et al. 1990) containing two pre-existing inclined flaws through the sample thickness. In all these cases, under uniaxial compression, a common cracking pattern is observed that involves wing and secondary cracks. According to Bobet (2000) these patterns occur through initiation of the wing cracks at the flaw tips followed by their propagation, in a curvilinear path, under increasing load with a tendency to align in the direction of the major principal stress. One of the most tests for investigating the fracture mechanism of rocks and rock-like specimens containing central pre-existing crack is Brazilian disc test (Ayatollahi and Aliha 2008; Wang 2010; Dai et al. 2010; Haeri et al. 2014 b, c, d). (Dai et al. 2011; Ayatollahi and Sistaninia 2011; Wang et al. 2011, 2012 ; Ghazvinian et al. 2013). (Awaji and Sato 1978; Sanchez 1979; Atkinson 1982; Shetty et al. 1986; Krishnan et al. 1998; Khan and Al-Shayea 2000 ; Al-Shayea et al. 2000 ; Al-Shayea 2005). Ghazvinian et al. (2013) carried out analytical, experimental, and numerical studies for detection of crack propagation in CSCBD specimens. Haeri et al. (2014d) studied the crack growth in pre-cracked rock-like disc specimens. Some computer codes were also used to simulate the failure mechanism of brittle materials, for example, Rock Failure Process Analysis (RFPA2D) code (Wong 2002), FROCK code (Park 2008), and 2D Particle Flow Code (PFC2D) (Lee and Manouchehrian et al. 2014). In the previous researches, a few center cracks have been considered

¹Department of Mining engineering, Hamedan university of technology, Mardom street, P.O.B. 65155-579

²Young Researchers and Elite Club, Bafgh Branch, Islamic Azad University, Bafgh, Iran

³Yazd University, Yazd

⁴College of Architecture and Environment, Sichuan University, Chengdu 610065, China

*Corresponding author, email: h.haeri@bafgh-iau.ac.ir

in the Brazilian disc specimens because it is usually difficult to produce specimens with multiple cracks in the laboratory. In this investigation, multiple cracks in the central part of the Brazilian discs are being analyzed numerically. The crack initiation stress, failure stress, the crack growth path, and crack coalescence have been studied. The numerical results were validated by experimental and numerical outputs developed by other research.

2 Bonded particle model and Particle Flow Code 2D (PFC2D)

Particle flow code in two dimensions (PFC2D) is a distinct element code that represents the material as an assembly of rigid particles which can move independently of one another and interact only at contacts (Itasca 1999 version 3.1; Potyondy and Cundall 2004). The movements and interaction forces of particles are calculated by use of a central finite difference method as applied in the DEM. For models of the contacts, both linear and non-linear contact models with frictional sliding can be used. The linear contact model, which was used in this study, provides an elastic relationship between the relative displacements and contact forces of particles. The basic contact model in the PFC code (contact force-displacement relationship) is the linear point contact between two particles (Fig. 1), relating contact normal force component, F^n , contact overlap, U^n , increment of shear force, ΔF^s , and shear displacements, ΔU^s , and given by:

$$\begin{cases} F^n = K^n U^n \\ \Delta F^s = -k^s \Delta U^s \end{cases} \quad (1)$$

where K^n and k^s are the contact normal and shear stiffness, respectively. The frictional strength of the contact is given by:

$$F^s \leq \mu F^n \quad (2)$$

where μ is the friction coefficient between particles. Point contact models represented by Eq. (1) can only consider relative motion between individual particles. However, when a group of bounded particles must be considered as a whole, cemented contact including both contact forces and torques are needed (Fig. 1). In such a case, the relationships between the above incremental quantities become:

$$\begin{cases} \Delta \bar{F}^n = k^n A \Delta U^n \\ \Delta \bar{F}^s = \bar{k}^s A \Delta U^s \end{cases} \quad (3)$$

And

$$\begin{cases} \Delta \bar{M}^n = k^s J \Delta U^n \\ \Delta \bar{M}^s = \bar{k}^n I \Delta U^s \end{cases} \quad (4)$$

Where ΔF^n , ΔF^s , ΔM^n and ΔM^s are the force components and torques (moments) about the center of the cemented-contact zone, k^n and k^s are normal and shear bond stiffness per unit

area, θ^n and θ^s are the components of rotation angle, and A , I , and J are the area, moment of inertia, and polar moment of inertia of the bond cross-section, respectively. The strength of the cemented contact is then written as:

$$\begin{aligned} \bar{\sigma}^{\max} &= \frac{-\bar{F}^n}{A} + \frac{|\bar{M}^s| \bar{R}}{I} < \bar{\sigma}_c \\ \bar{\tau}^{\max} &= \frac{-\bar{F}^s}{A} + \frac{|\bar{M}^n| \bar{R}}{J} < \bar{\tau}_c \end{aligned} \quad (5)$$

Where R is the radius of the cemented zone (Fig. 1), σ_c and τ_c are the tensile and shear strength of the cemented contact, respectively. Young's modulus for particle contacts E_c and particle bondage \bar{E}_c are defined to relate the contact and bond stiffness as follows:

$$\begin{aligned} E_c &= \frac{k_n}{2t} (t = 1in2D) \\ \bar{E}_c &= \bar{k}_n (R^{(A)} + R^{(B)}) \end{aligned} \quad (6)$$

where $R^{(A)}$ and $R^{(B)}$ are radii of circular particles in contact (Fig. 1). In the PFC code, cemented contacts as expressed in Eqs. (3)–(8) are called parallel bonds. By using the parallel bond model it is possible to reproduce the mechanical properties of a rock-like material.

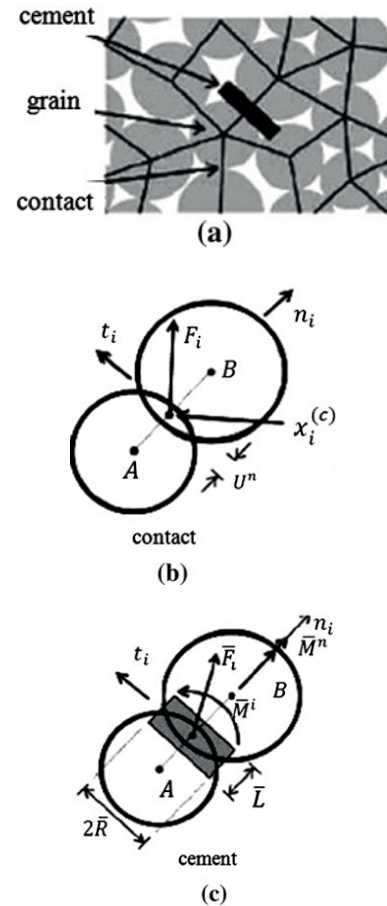


Fig. 1 Contact and cement in PFC.

To generate a parallel-bonded particle model for PFC2D, using the routines provided (Itasca 1999; version 3.1), the following micro properties should be defined: ball-to-ball contact modulus, stiffness ratio k_n over k_s , ball friction coefficient, parallel normal bond strength, parallel shear bond strength, ratio of standard deviation to mean of bond strength both in normal and shear direction, minimum Ball radius, parallel-bond radius multiplier, parallel-bond modulus, and parallel-bond stiffness ratio. To establish the appropriate micro properties to be used for the particle assembly, it is necessary to conduct a calibration procedure. The particle contact properties and bonding characteristics cannot be determined directly from tests performed on laboratory model samples. The material properties determined by laboratory experimentation are macro-mechanical in nature because they reflect continuum behaviour. An inverse modelling procedure was used to determine the appropriate micro-mechanical properties of the numerical models from the macro-mechanical properties determined in the laboratory tests. The trial-and-error approach is one of the methods used to relate these two sets of material property (Itasca 1999). It involves assumption of micro-mechanical property values and comparison of the strength and deformation characteristics of the numerical models with those of the laboratory samples. The micro-mechanical property values that give a simulated macroscopic response close to that of the laboratory tests are then adopted for the discontinuous jointed blocks.

2.1 Preparing and Calibrating the Numerical Model

The Brazilian test was used to calibrate the tensile strength of specimen in PFC2D model. The standard process of generation of a PFC2D assembly to represent a test model involves four steps: (a) particle generation and packing the particles, (b) isotropic stress installation, (c) floating particle elimination, and (d) bond installation.

Adopting the micro-properties listed in Table 1 and the standard calibration procedures (Potyondy and Cundall, 2003), a calibrated PFC particle assembly was created. The diameter of the Brazilian disk considered in the numerical tests was 54 mm. The specimen was made of 5,615 particles. The disk was crushed by the lateral walls moved toward each other with a low speed of 0.016 m/s. Figures 2 a, b illustrate the failure patterns of the numerical and experimental tested samples, respectively. Also displacement vector of particle and bond force distribution was shown in Fig. 2 b. The failure planes experienced in numerical and laboratory tests are well matching. The numerical tensile strength and a comparison of its experimental measurements were presented in Table 2. This table shows a good accordance between numerical and experimental results.

Table 1 Micro properties used to represent the intact rock

Parameter	Value	Parameter	Value
Type of particle	disc	Parallel bond radius multiplier	1
density	3000	Young modulus of parallel bond (GPa)	40
Minimum radius	0.27	Parallel bond stiffness ratio	1.7
Size ratio	1.56	Particle friction coefficient	0.4
Porosity ratio	0.08	Parallel bond normal strength, mean (MPa)	7
Damping coefficient	0.7	Parallel bond normal strength, SD (MPa)	2
Contact young modulus (GPa)	40	Parallel bond shear strength, mean (MPa)	7
Stiffness ratio	1.7	Parallel bond shear strength, SD (MPa)	2

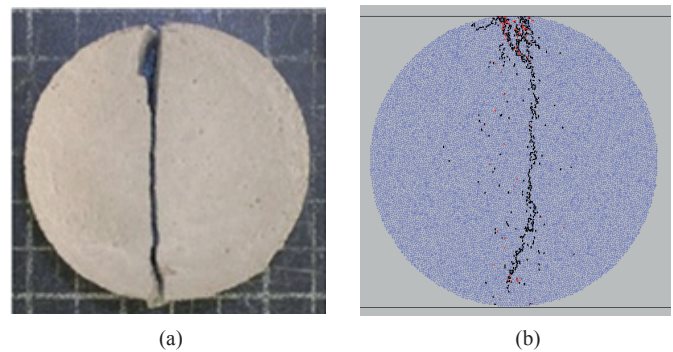


Fig. 2 failure pattern in a) physical sample, b) PFC2D model.

Table 2 Brazilian tensile strength of physical and numerical samples.

Physical tensile strength (MPa)	1.5 and 1.7
Numerical tensile strength (MPa)	1.5

2.2 Model preparation using Particle Flow Code

After calibration of PFC2D, Brazilian tensile tests were simulated by creating a circular model in PFC2D (by using the calibrated micro-parameters) (Fig. 3).

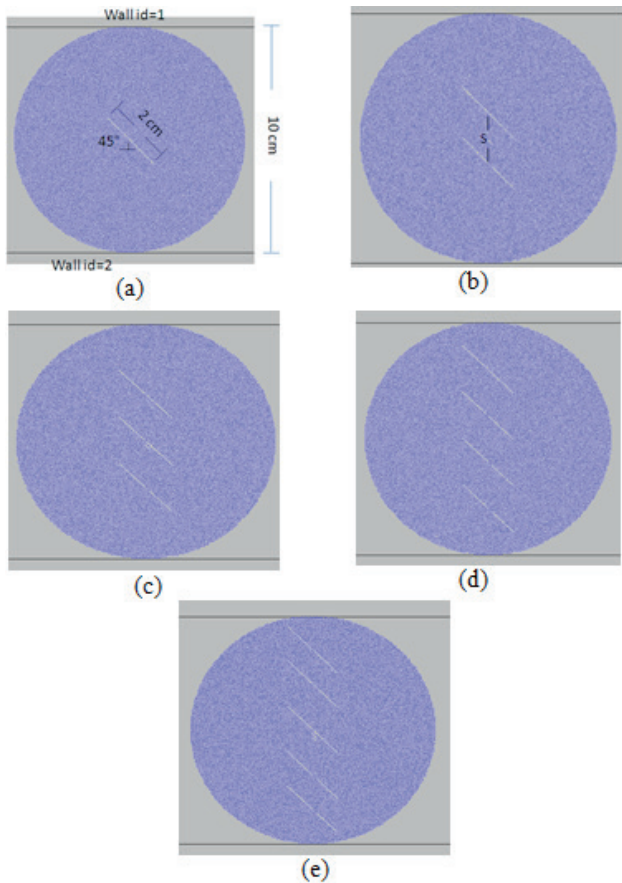


Fig. 3 Different types of vertically cracks, a) one notch, b) two notch, c) three notch, d) four notch and e) five notch.

The PFC specimen had diameter of 100 mm. A total of 14,179 disks with a minimum radius of 0.27 mm were used to make up the Brazilian specimen. Brazilian discs contain one, two, three, four, and five parallel centred cracks. These notches distributed vertically (Fig. 3) and horizontally in the model (Fig. 4). The notch lengths were 2cm. The vertical spacing (s) between notches was 2 cm. Angularity of all notches related to horizontal line was 45° . Models containing two and three cracks have different joint spacing (i.e. $s = 2$ cm, 3 cm and 4 cm in Fig. 5) and distributed horizontally (Fig. 5 and Fig. 6) and vertically (Fig. 7 and Fig. 8) in the model. This flaw geometry is different from those reported in the previous studies, where only one flaw was used. The model was crushed by lateral walls moved toward each other. The Tensile force and crack initiation force were registered by taking the reaction forces on the wall 1 in Fig. 7 c.

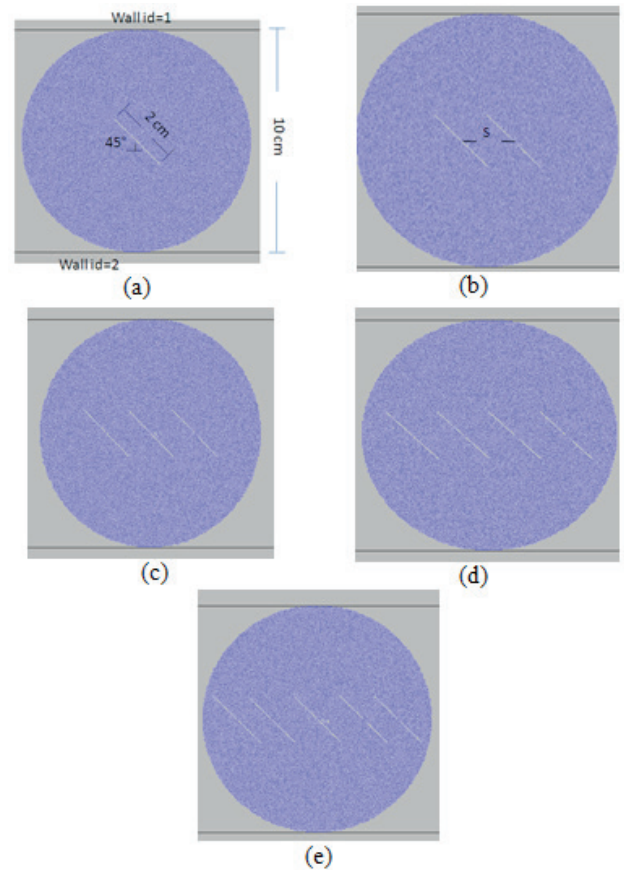


Fig. 4 Different types of horizontally cracked models consisting, a) one notch, b) two notch, c) three notch, d) four notch and e) five notch.

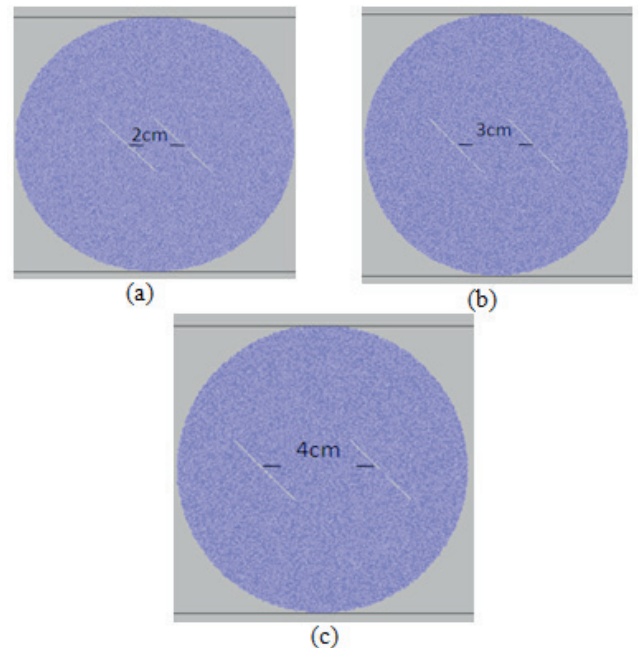


Fig. 5 Horizontally cracks with spacing of, a) 2cm, b) 3 cm, c) 4 cm.

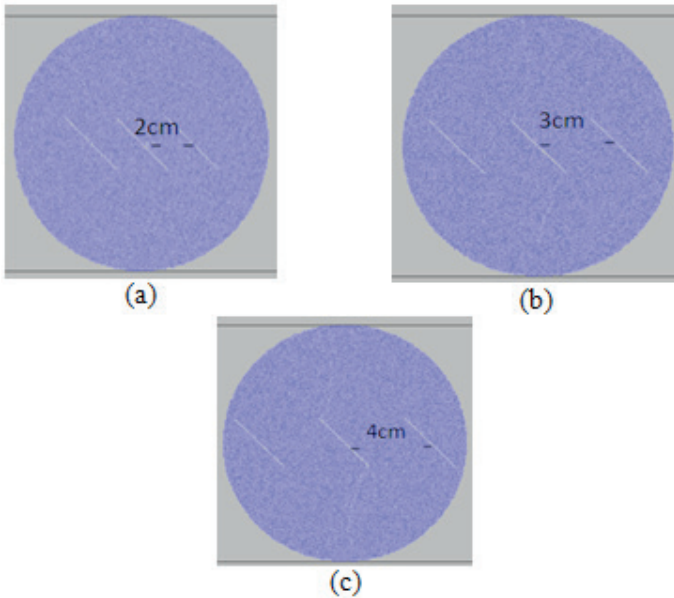


Fig. 6 horizontally cracks with spacing of, a) 2cm, b) 3 cm, c) 4 cm.

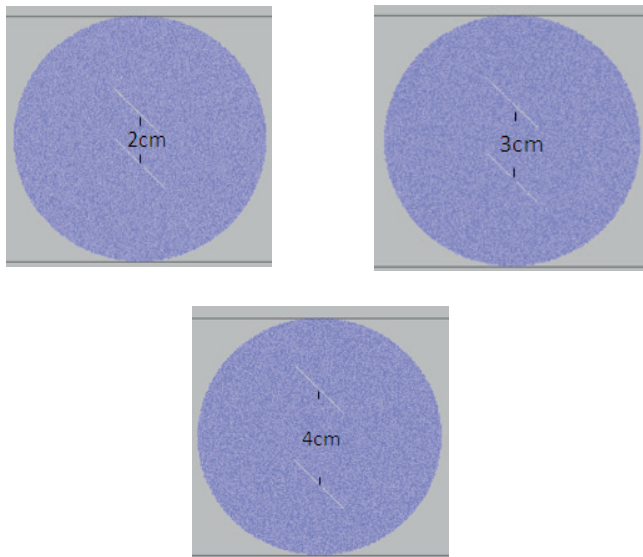


Fig. 7 vertically cracks with spacing of, a) 2cm, b) 3 cm, c) 4 cm.

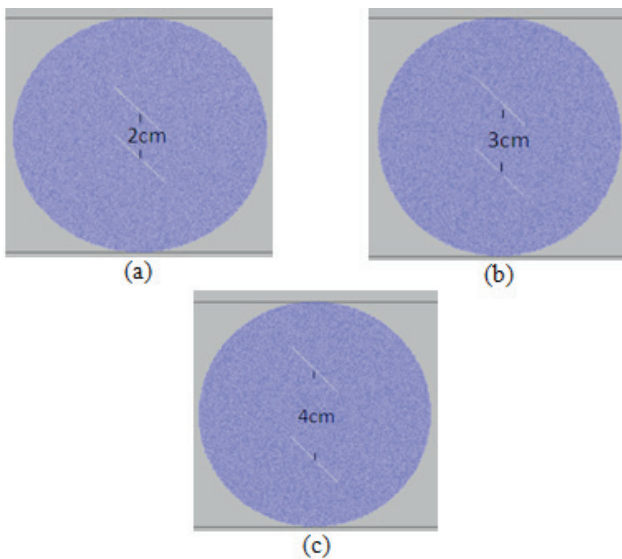


Fig. 8 vertically cracks with spacing of, a) 2cm, b) 3 cm, c) 4 cm.

3 Results

3.1 Effect of number of notches on the failure mechanism of model

Fig. 9 a–e shows the effect of number of notches, vertically distributed in the models, on the failure mechanism of model.

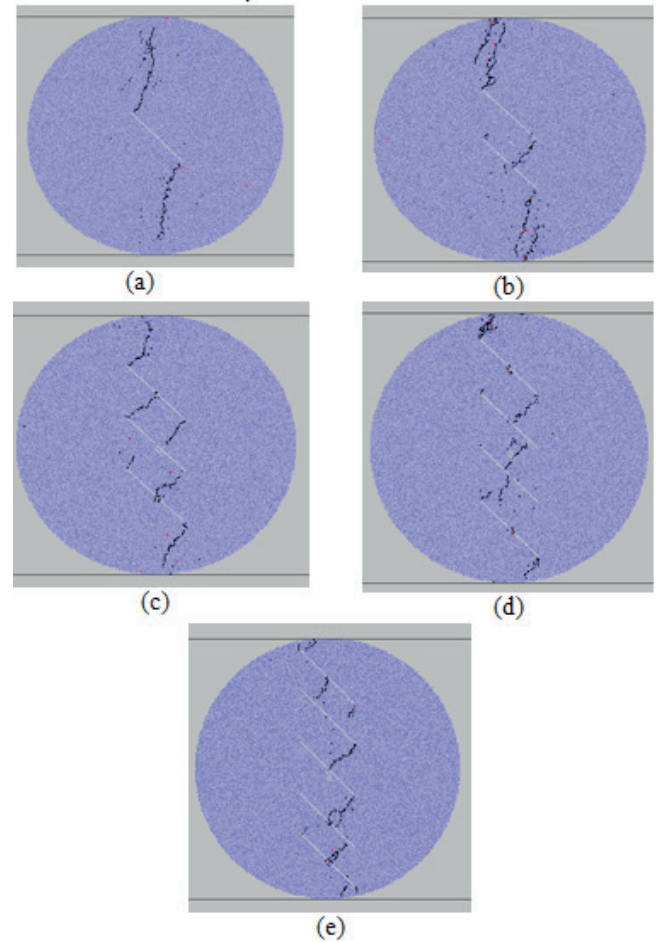


Fig. 9 fracturing path in model containing a) single notch, b) two parallel notch, c) three parallel notch, d) four parallel notch, and e) five parallel notch.

When one notch exist in the model, tensile cracks initiate from the notch tips and propagates parallel to loading axis till coalesce with edge of the model. When two, three, four and five notches exist in the model, outer tensile cracks initiate from the notch tips and propagates parallel to loading axis till coalesce with edge of the model. The inner tensile cracks initiate from middle of the lower notches and propagate diagonally till coalesce with tip of the upper joint (Fig. 9 a,b,c,d).

As can be observed by comparing between Fig. 9 and Fig. 10, there is good accordance between numerical simulation and experimental results obtained by haeri et al. (2014).

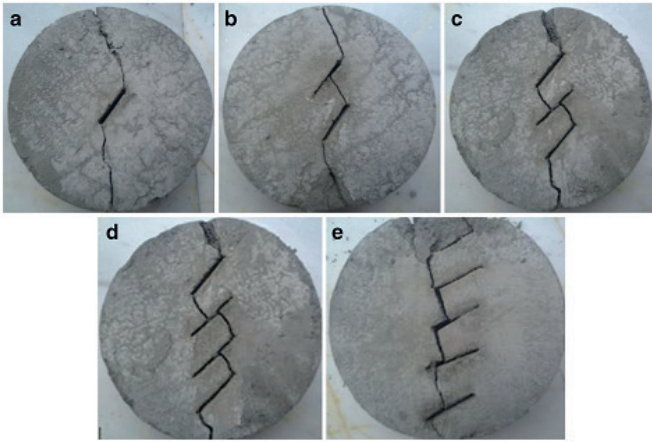


Fig. 10 Experimental results illustrating the fracturing path of rock-like disc specimens containing a) single crack, b) two parallel cracks, c) three parallel cracks, d) four parallel cracks, and e) five parallel cracks.

Haeri et al (2014) simulate numerically crack propagation in notched Brazilian disc with same notch configuration. Comparison between Fig. 9 and Fig. 11, shows that the simulated propagation paths are in good agreement with the corresponding high order DDM numerical results obtained by Haeri et al (2014).

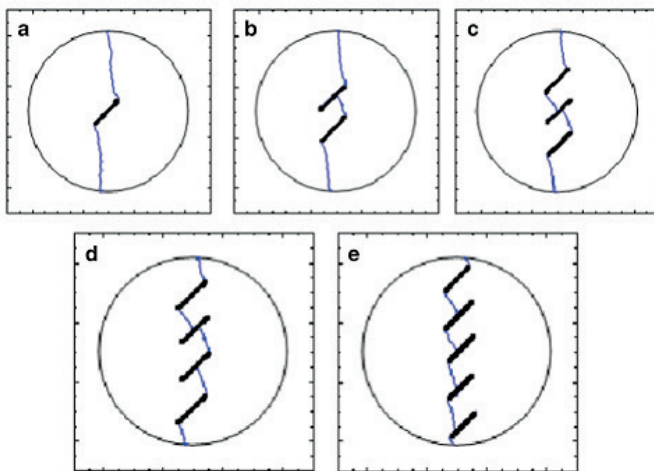


Fig. 11 Numerical simulation of the crack propagation path for pre-cracked Brazilian disc specimens containing a) single crack, b) two parallel cracks, c) three parallel cracks, d) four parallel cracks, and e) five parallel cracks with a constant spacing, notch length is 20 mm.

Fig. 12 a–e shows the effect of number of notches, horizontally distributed in the models, on the failure mechanism of numerical model. When one, three and five notch exist in the model, tensile cracks initiate from the notch tips and propagates parallel to loading axis till coalesce with edge of the model (Figs. 12a, c and e). When two and four notches exist in the model, outer tensile cracks initiate from the notch tips and propagates parallel to loading axis till coalesce with edge of the model. Also, two major tensile fractures form between two interior notches. This fractures initiates from middle of the notch and coalesce with tip of the other notch (Fig. 12b,d). in

other word when notch exist in symmetrical line of Brazilian model, cracks growth from middle notch but when notches exist in both sides of symmetrical line, cracks growth from double notches situated in middle parts.

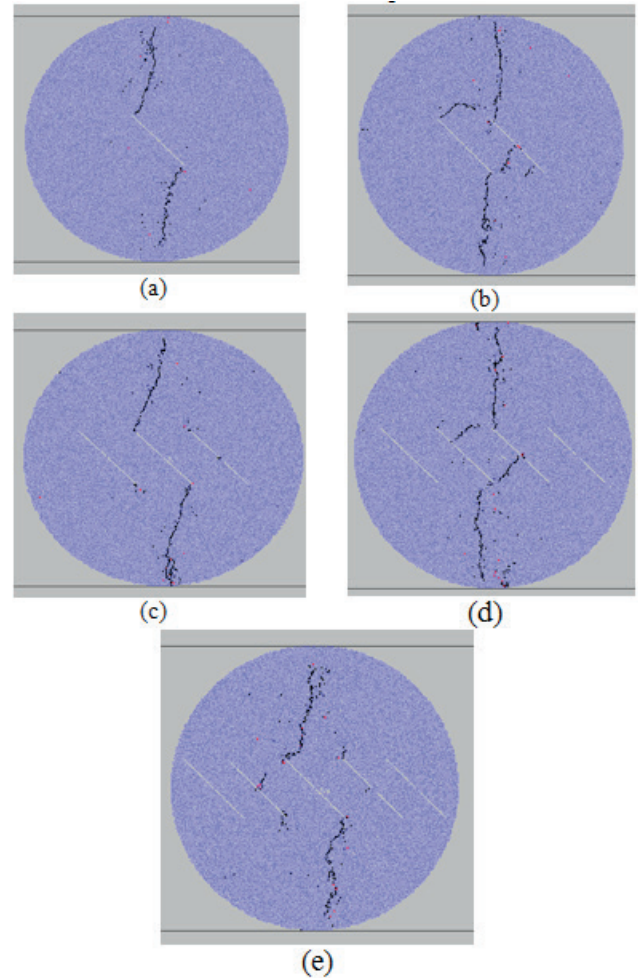


Fig. 12 fracturing path in models containing a) single notch, b) two parallel notch, c) three parallel notch, d) four parallel notch, and e) five parallel notch.

Fig. 13 a–c shows the effect of spacing between two notches, horizontally distributed in the models, on the failure mechanism of numerical model. When notch spacing is 1cm, outer tensile cracks initiate from the notch tips and propagates parallel to loading axis till coalesce with edge of the model. Also, two major tensile fractures form between two interior notches. This fractures initiates from middle of the notch and coalesce with tip of the other notch (Fig. 11a). When notch spacing is 2cm, outer tensile cracks initiate from the notch tips and propagates parallel to loading axis till coalesce with edge of the model. Also, one major tensile fractures initiate from upper tip of the notch and propagate vertically till coalesces with lower tip of the other notch (Fig. 11b). When notch spacing is 3cm, outer tensile cracks initiate from the notch tips and propagates parallel to loading axis till coalesce with edge of the model. Also, two major tensile fractures initiates from upper tip of the left notch and lower tip of the right notch and propagate diagonally till coalesce with loading area (Fig. 11c).

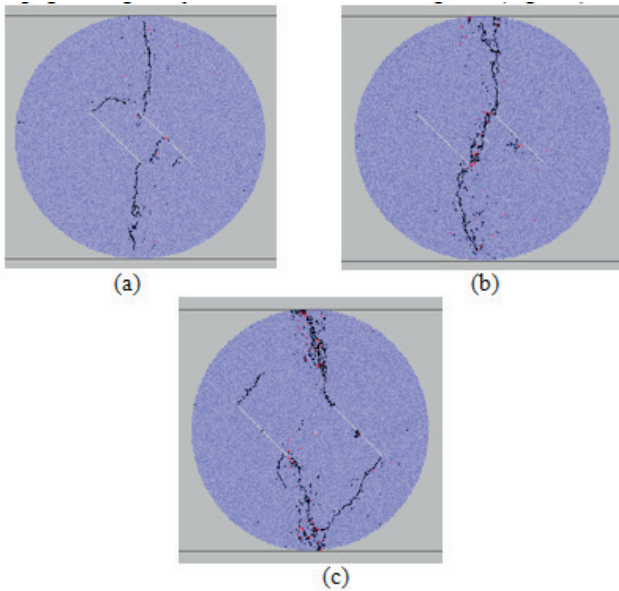


Fig. 13 fracturing path in models containing a) single notch, b) two parallel notch, c) three parallel notch, d) four parallel notch, and e) five parallel notch.

Fig. 13 a–c shows the effect of spacing between three notches, horizontally distributed in the models, on the failure mechanism of numerical model. When notch spacing is 1cm, 2cm and 3cm, outer tensile cracks initiate from the middle notch tips and propagates parallel to loading axis till coalesce with edge of the model. Number of total cracks was increased by increasing the notch spacing. Also several bands of cracks initiates from loading places.

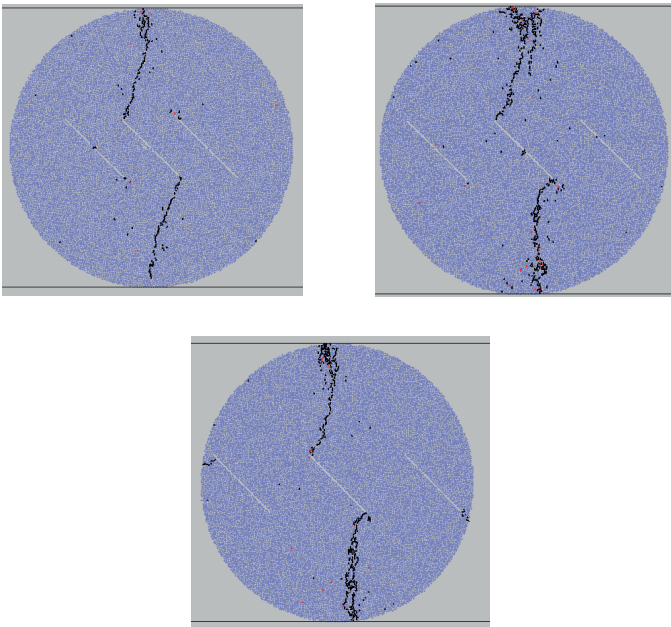


Fig. 14 fracturing path in different model containing a) single notch, b) two parallel notch, c) three parallel notch, d) four parallel notch, and e) five parallel notch.

Fig. 14 a–c shows the effect of spacing between two notches, vertically distributed in the models, on the failure mechanism of numerical model. When notch spacing is 1cm, 2cm and 3 cm, outer tensile cracks initiate from the notch tips and propagates

parallel to loading axis till coalesce with edge of the model. Also, one major tensile fractures form between two interior notches. This fractures initiates from middle of the notch and coalesce with tip of the other notch. Direction of this fracture is perpendicular to notch length.

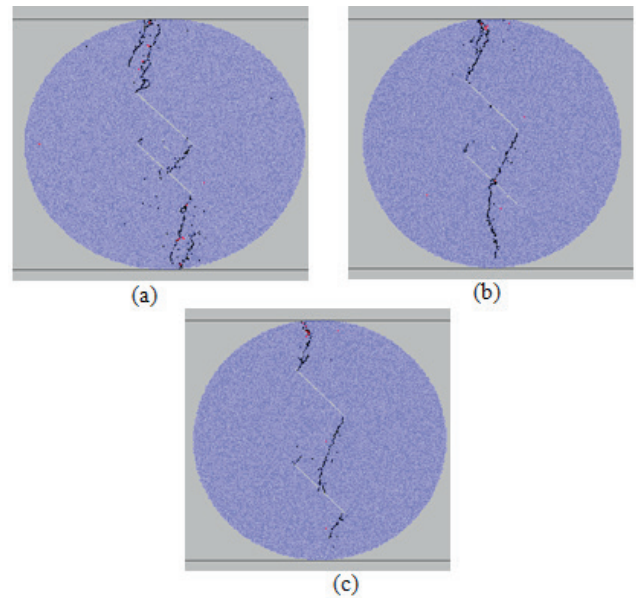


Fig. 15 fracturing path of disc model containing a) single notch, b) two parallel notch, c) three parallel notch, d) four parallel notch, and e) five parallel notch.

Haeri et al (2014) simulate numerically crack propagation in notched Brazilian disc with same notch configuration. Comparison between Fig. 14 and Fig. 15, shows that the simulated propagation paths are in good agreement with the corresponding high order DDM numerical results obtained by Haeri et al (2014).

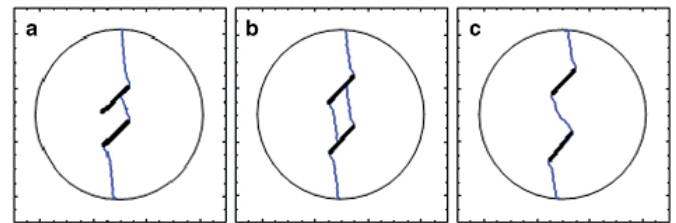


Fig. 16 Numerical simulation of the crack propagation path for Brazilian disc specimens containing two parallel cracks (the inclination angle of crack, $\beta = 45^\circ$) for different spacing: a) $S = 20$ mm, b) $S = 30$ mm, and c) $S = 40$ mm, Haeri et al (2014)

Fig. 16 a–c shows the effect of spacing between three notches, vertically distributed in the models, on the failure mechanism of numerical model. When notch spacing is 1cm, 2cm and 3cm, outer tensile cracks initiate from the notch tips and propagates parallel to loading axis till coalesce with edge of the model. Also, two major tensile fractures form between two interior notches. These fractures initiate from middle of the one notch and coalesce with tip of the other notch. Direction of this fracture is perpendicular to notch length.

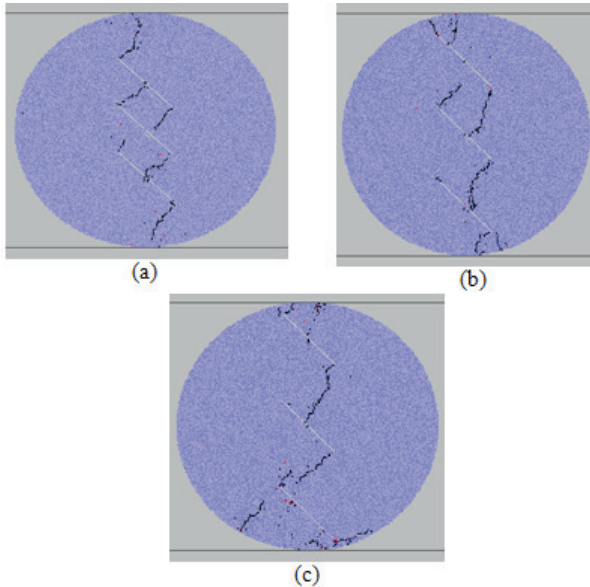


Fig. 17 fracturing path in models containing a) single notch, b) two parallel notch, c) three parallel notch, d) four parallel notch, and e) five parallel notch.

Haeri et al (2014) simulate numerically crack propagation in notched Brazilian disc with same notch configuration. Comparison between Fig. 17 and Fig. 18 shows that the simulated propagation paths are in good agreement with the corresponding high order DDM numerical results obtained by Haeri et al (2014).

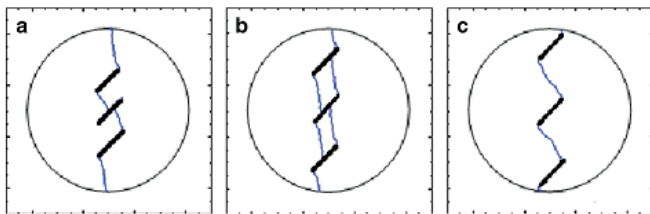


Fig. 18 Numerical simulation of the crack propagation path for Brazilian disc specimens containing two parallel cracks (the inclination angle of crack, $\beta = 45^\circ$) for different spacing: a) $S = 20$ mm, b) $S = 30$ mm, and c) $S = 40$ mm, Haeri et al (2014).

3.2 The effect of notch number on the failure stress and crack initiation stress

Fig. 19 a and b shows the effect of number of notch on the critical stresses for vertically and horizontally distributed notches in the model, respectively. The results of failure stress and crack initiation stress were depicted in these figures. When notches distributed vertically in the model, both of the crack initiation stress and failure stresses decreases by increasing the joint number. In this configuration, all of the joints were mobilized in failure process and led to decreasing the strength of model. But, when notches distributed horizontally in the model, both of the crack initiation stress and failure stresses were increased by increasing the joint spacing. In this configuration, number of shear cracks increased by increasing the joint spacing. This led to increasing the strength of model. But, when notches distributed vertically in the model, both of the crack initiation stress and failure stresses were decreased by increasing the joint spacing. In this configuration, joints are closed to loading place with increasing the joint spacing. This led to decreasing the strength of model. Its to be note that in all configuration, all joints mobilized in failure process.

initiates only from middle notch but two notches mobilized in failure process when two and four notches exist in numerical model. This led to non-homogeneity between failure strength and crack initiation of numerical models.

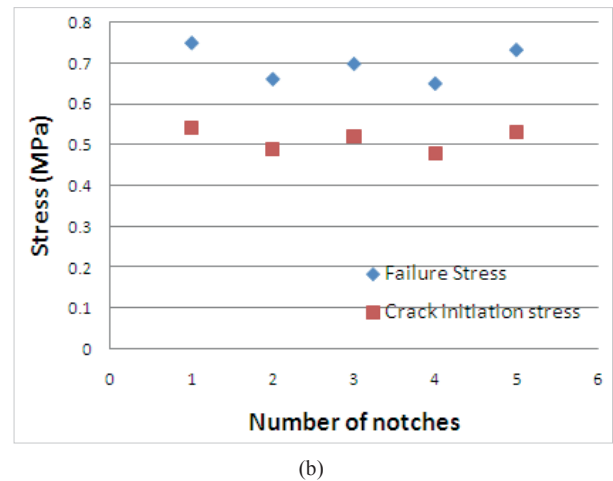
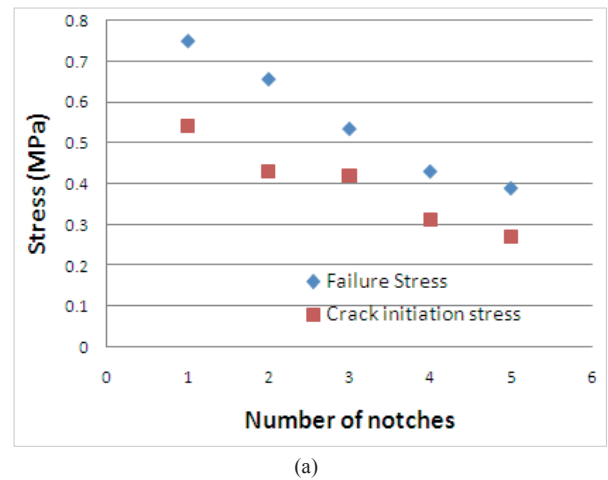
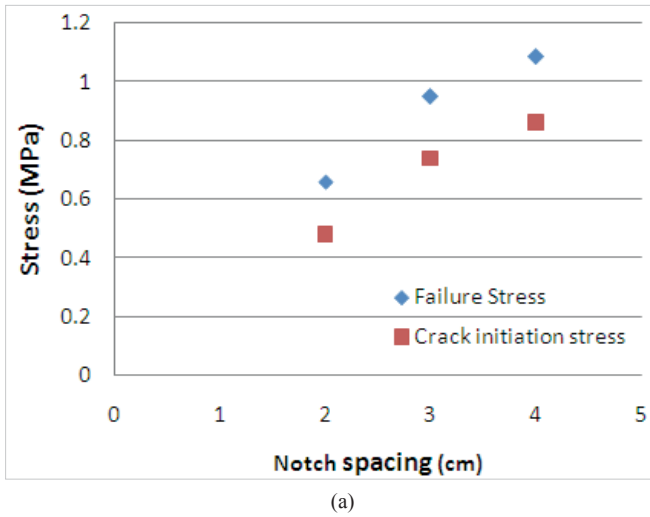
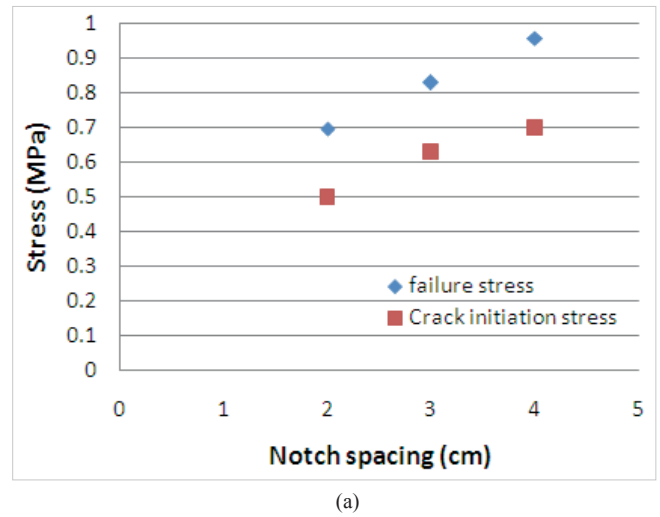


Fig. 19 the effect of number of notch on the critical stresses for a) vertically notches in the model, b) horizontally notches in the model.

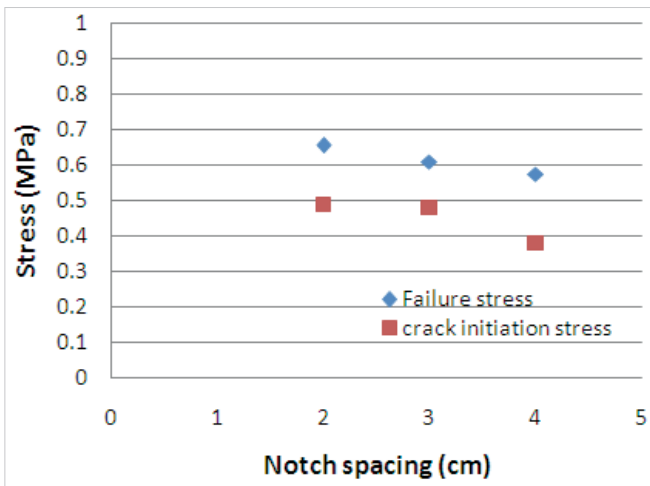
Fig. 20 a and b shows the effect of notch spacing on the critical stresses for vertically and horizontally distribution of two notches in the model, respectively. The results of failure stress and crack initiation stress were depicted in these figures. When notches distributed horizontally in the model, both of the crack initiation stress and failure stresses increases by increasing the joint spacing. In this configuration, number of shear cracks increased by increasing the joint spacing. This led to increasing the strength of model. But, when notches distributed vertically in the model, both of the crack initiation stress and failure stresses were decreased by increasing the joint spacing. In this configuration, joints are closed to loading place with increasing the joint spacing. This led to decreasing the strength of model. Its to be note that in all configuration, all joints mobilized in failure process.



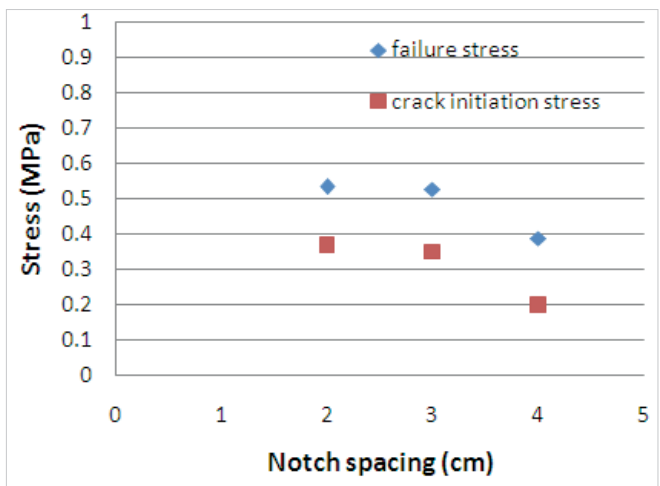
(a)



(a)



(b)



(b)

Fig. 20 Effect of notch spacing on critical stresses in, a) vertically notches in the model, b) horizontally notches in the model.

Fig. 21 Effect of notch spacing on critical stresses in, a) vertically distribution of three notches in the model, b) horizontally distribution of three notches in the model.

Fig. 21 a and b shows the effect of notch spacing on the critical stresses for vertically and horizontally distribution of three notches in the model, respectively. The results of failure stress and crack initiation stress were depicted in these figures. When notches distributed horizontally in the model, both of the crack initiation stress and failure stresses increases by increasing the joint spacing. In this configuration, the effect of two neighbouring joints on the stress distribution around the middle joint decreased by increasing the joint spacing. This led to increasing the number of total cracks and increasing the strength of model. But, when notches distributed vertically in the model, both of the crack initiation stress and failure stresses were decreased by increasing the joint spacing. In this configuration, joints are closed to loading place with increasing the joint spacing. This led to decreasing the strength of model. Its to be note that in this configuration, all joints mobilized in failure process.

4 Conclusions

In this research, multiple parallel cracks in the central part of the Brazilian discs are simulated numerically using PFC2D. These multiple center cracks are produced so that they would be parallel with each other. The failure stress, crack initiation stress, crack propagation, and crack coalescence through the models and in the bridge area (the areas in between the parallel multiple cracks) have been investigated. The numerical models well illustrate the production of the wing cracks and the crack propagation paths produced by the coalescence phenomenon of the multiple pre-existing parallel cracks in the bridge area.

When two notches distributed horizontally in the model, both of the crack initiation stress and failure stresses increases by increasing the joint spacing. In this configuration, number of shear cracks increased by increasing the joint spacing. This led to increasing the strength of model. But, when notches distributed vertically in the model, both of the crack initiation stress and failure stresses were decreased by increasing the joint spacing. In this configuration, joints are closed to loading place with increasing the joint spacing. This led to decreasing

the strength of model. Its to be note that in all configuration, all joints mobilized in failure process. When three notches distributed horizontally in the model, both of the crack initiation stress and failure stresses increases by increasing the joint spacing. In this configuration, the effect of two neighbouring joints on the stress distribution around the middle joint decreased by increasing the joint spacing. This led to increasing the number of total cracks and increasing the strength of model. But, when notches distributed vertically in the model, both of the crack initiation stress and failure stresses were decreased by increasing the joint spacing. In this configuration, joints are closed to loading place with increasing the joint spacing. This led to decreasing the strength of model. Its to be note that in this configuration, all joints mobilized in failure process.

These numerical results are compared with other research results and it has been shown that there is a good agreement between them which demonstrates the accuracy and validity of the present analyses. The preference of PFC is that it can reduce computation efforts. The simulation is easy and it is not necessary to define crack tips location where stress concentrates. In PFC2d, it is possible to see branching in the model while only one single crack is identifiable in DDM method. Simple formulation is used in structure of PFC2D while DDM has complicate formula.

More flexibility in the analysis can be achieved by using the proposed numerical method so that it may be possible to investigate the effects of bridge area and orientation of cracks on the breakage process of pre-cracked disc specimens with multiple parallel cracks. These numerical results are expected to improve the understanding of the characteristics of crack growth and crack coalescence and can be used to analyze the stability of rock and rock structures, such as the excavated underground openings or slopes, tunneling construction, where pre-existing cracks or fractures play a crucial role in the overall integrity of such structures.

References

- [1] Al-Shayea, N. A. "Crack propagation trajectories for rocks under mixed mode I-II fracture." *Engineering Geology*, 81(1), pp. 84–97. 2005. [10.1016/j.enggeo.2005.07.013](https://doi.org/10.1016/j.enggeo.2005.07.013)
- [2] Al-Shayea, N. A., Khan, K., Abduljawwad, S. N. "Effects of confining pressure and temperature on mixed-mode (I-II) fracture toughness of a limestone rock formation." *International Journal of Rock Mechanics and Mining Sciences*, 37(4), pp. 629–643. 2000. [10.1016/S1365-1609\(00\)00003-4](https://doi.org/10.1016/S1365-1609(00)00003-4)
- [3] Atkinson, C., Smelser, R. E., Sanchez, J. "Combined mode fracture via the cracked Brazilian disk." *International Journal of Fracture*, 18(4), pp. 279–291. 1982. [10.1007/BF00015688](https://doi.org/10.1007/BF00015688)
- [4] Awaji, H., Sato, S. "Combined mode fracture toughness measurement by the disk test." *Journal of Engineering Materials and Technology*, 100(2), pp. 175–182. 1978. [10.1115/1.3443468](https://doi.org/10.1115/1.3443468)
- [5] Ayatollahi, M. R., Aliha, M. R. M. "On the use of Brazilian disc specimen for calculating mixed mode I–II fracture toughness of rock materials." *Engineering Fracture Mechanics*, 75(16), pp. 4631–4641. 2008. [10.1016/j.engfracmech.2008.06.018](https://doi.org/10.1016/j.engfracmech.2008.06.018)
- [6] Ayatollahi, M. R., Sistaninia, M. "Mode II fracture study of rocks using Brazilian disk specimens." *International Journal of Rock Mechanics and Mining Sciences*, 48(5), pp. 819–826. 2011. [10.1016/j.ijrmms.2011.04.017](https://doi.org/10.1016/j.ijrmms.2011.04.017)
- [7] Bobet, A., Einstein, H. H. "Fracture coalescence in rock-type materials under uniaxial and biaxial compression." *International Journal of Rock Mechanics and Mining Sciences*, 35(7), pp. 863–888. 1998. [10.1016/S0148-9062\(98\)00005-9](https://doi.org/10.1016/S0148-9062(98)00005-9)
- [8] Bobet, A. "The initiation of secondary cracks in compression." *Engineering Fracture Mechanics*, 66(2), pp. 187–219. 2000. [10.1016/S0013-7944\(00\)00009-6](https://doi.org/10.1016/S0013-7944(00)00009-6)
- [9] Dai, F., Xia, K., Zheng, H., Wang, Y. X. "Determination of dynamic rock mode-I fracture parameters using cracked chevron notched semi-circular bend specimen." *Engineering Fracture Mechanics*, 78, pp. 2633–2644. 2011.
- [10] Dai, F., Chen, R., Iqbal, M. J., Xia, K. "Dynamic cracked chevron notched Brazilian disc method for measuring rock fracture parameters." *International Journal of Rock Mechanics and Mining Sciences*, 47(4), pp. 606–613. 2010. [10.1016/j.ijrmms.2010.04.002](https://doi.org/10.1016/j.ijrmms.2010.04.002)
- [11] Ghazvinian, A., Nejati, H. R., Sarfarazi, V., Hadei, M. R. "Mixed mode crack propagation in low brittle rock-like materials." *Arabian Journal of Geosciences*, 6(11), pp. 4435–4444. 2013. [10.1007/s12517-012-0681-8](https://doi.org/10.1007/s12517-012-0681-8)
- [12] Krishnan, G. R., Zhao, X. L., Zaman, M., Rogiers, J. C. "Fracture toughness of a soft sandstone." *International Journal of Rock Mechanics and Mining Sciences*, 35(6), pp. 695–710. 1998. [10.1016/S0148-9062\(97\)00324-0](https://doi.org/10.1016/S0148-9062(97)00324-0)
- [13] Khan, K., Al-Shayea, N. A. "Effects of specimen geometry and testing method on mixed-mode I–II fracture toughness of a limestone rock from Saudi Arabia." *Rock Mechanics and Rock Engineering*, 33(3), pp. 179–206. 2000. [10.1007/s006030070006](https://doi.org/10.1007/s006030070006)
- [14] Haeri, H., Khaloo, A., Marji, M. F. "Experimental and numerical analysis of Brazilian discs with multiple parallel cracks." *Arabian Journal of Geosciences*, 8(8), pp. 5897–5908. 2015. [10.1007/s12517-014-1598-1](https://doi.org/10.1007/s12517-014-1598-1)
- [15] Haeri, H., Shahriar, K., Marji, M. F., Moarefvand, P. "Experimental and numerical study of crack propagation and coalescence in pre-cracked rock-like disks." *International Journal of Rock Mechanics and Mining Sciences*, 67, pp. 20–28. 2014. [10.1016/j.ijrmms.2014.01.008](https://doi.org/10.1016/j.ijrmms.2014.01.008)
- [16] Haeri, H., Marji, M. F., Shahriar, K., Moarefvand, P. "On the HDD analysis of micro cracks initiation, propagation, and coalescence in brittle materials." *Arabian Journal of Geosciences*, 8(59), pp. 2841–2852. 2015. [10.1007/s12517-014-1290-5](https://doi.org/10.1007/s12517-014-1290-5)
- [17] Haeri, H., Shahriar, K., Marji, M. F., Moarefvand, P. "On the crack propagation analysis of rock like Brazilian disc specimens containing cracks under compressive line loading." *Latin American Journal of Solids and Structures*, 11(8), pp. 400–416. 2014. [10.1590/S1679-78252014000800007](https://doi.org/10.1590/S1679-78252014000800007)
- [18] Ingraffea, A. R., Heuze, F. E. "Finite element models for rock fracture mechanics." *International Journal for Numerical and Analytical Methods in Geomechanics*, 4(1), pp. 25–43. 1980. [10.1002/nag.1610040103](https://doi.org/10.1002/nag.1610040103)
- [19] Jiefan, H., Ganglin, C., Yonghong, Z., Ren, W. "An experimental study of the strain field development prior to failure of a marble plate under compression." *Tectonophysics*, 175(1–3), pp. 269–284. 1990. [10.1016/0040-1951\(90\)90142-U](https://doi.org/10.1016/0040-1951(90)90142-U)
- [20] Park, C. H. "Coalescence of frictional fractures in rock materials." PhD Thesis, Purdue University West Lafayette, Indiana. 2008.
- [21] Petit, J., Barquins, M. "Can natural faults propagate under mode II conditions?" *Tectonics*, 7(6), pp. 1243–1256. 1988. [10.1029/TC007i006p01243](https://doi.org/10.1029/TC007i006p01243)
- [22] Reyes, O., Einstein, H. H. "Failure mechanism of fractured rock - a fracture coalescence model." In: Proceedings 7th International Congress of Rock Mechanics. pp. 333–340. 1991.

- [23] Sanchez, J. "Application of the disk test to mode-I-II fracture toughness analysis." M S Thesis, Department of Mechanical Engineering, University of Pittsburgh, Pittsburgh, U.S.A. 1979.
- [24] Scavia, C., Castelli, M. "Studio della propagazione per trazione indotta di sistemi di fratture in roccia." *Rivista Italiana di Geotecnica*, XXXII, pp. 48–62. 1998. (In Italian)
- [25] Shen, B., Stephansson, O. "Large-scale permeability tensor of rocks from induced microseismicity." *International Journal of Rock Mechanics and Mining Sciences*, 30, pp. 861–867. 1993.
- [26] Shen, B., Stephansson, O., Einstein, H. H., Ghahreman, B. "Large-scale permeability tensor of rocks from induced micro-seismicity." *Journal of Geophysical Research*, 100, pp. 5975–5990. 1995.
- [27] Shetty, D. K., Rosenfield, A. R., Duckworth, W. H. "Mixed-mode fracture of ceramics in diametrical compression." *Journal of the American Ceramic Society*, 69(6), pp. 437–443. 1986. [10.1111/j.1151-2916.1986.tb07441.x](https://doi.org/10.1111/j.1151-2916.1986.tb07441.x)
- [28] Mughieda, O., Alzoubi, K. A. "Fracture mechanisms of offset rock joints — A laboratory investigation." *Geotechnical & Geological Engineering*, 22(4), pp. 545–562. 2004. [10.1023/B:GEGE.0000047045.89857.06](https://doi.org/10.1023/B:GEGE.0000047045.89857.06)
- [29] Manouchehrian, A., Sharifzadeh, M., Marji, M. F., Gholamnejad, J. "A bonded particle model for analysis of the flaw orientation effect on crack propagation mechanism in brittle materials under compression." *Archives of Civil Mechanical Engineering*, 14(81), pp. 40–52. 2014. [10.1016/j.acme.2013.05.008](https://doi.org/10.1016/j.acme.2013.05.008)
- [30] Haeri, H., Khaloo, A., Marji, M. F. "Experimental and numerical analysis of Brazilian discs with multiple parallel cracks." *Arabian Journal of Geosciences*, 8(8), pp. 5897–5908. 2015. DOI: [10.1007/s12517-014-1598-1](https://doi.org/10.1007/s12517-014-1598-1)
- [31] Wang, Q. Z. "Formula for calculating the critical stress intensity factor in rock fracture toughness tests using cracked chevron notched Brazilian disc (CCNBD) specimens." *International Journal of Rock Mechanics and Mining Sciences*, 47(6), pp. 1006–1011. 2010. [10.1016/j.ijrmms.2010.05.005](https://doi.org/10.1016/j.ijrmms.2010.05.005)
- [32] Wang, Q. Z., Feng, F., Ni, M., Gou, X. P. "Measurement of mode I and mode II rock dynamic fracture toughness with cracked straight through flattened Brazilian disc impacted by split Hopkinson pressure bar." *Engineering Fracture Mechanics*, 78(12), pp. 2455–2469. 2011. [10.1016/j.engfracmech.2011.06.004](https://doi.org/10.1016/j.engfracmech.2011.06.004)
- [33] Wang, Q. Z., Gou, X. P., Fan, H. "The minimum dimensionless stress intensity factor and its upper bound for CCNBD fracture toughness specimen analyzed with straight through crack assumption." *Engineering Fracture Mechanics*, 82, pp. 1–8. 2012. [10.1016/j.engfracmech.2011.11.001](https://doi.org/10.1016/j.engfracmech.2011.11.001)
- [34] Wong, R. H. C., Tang, C. A., Chau, K. T., Lin, P. "Splitting failure in brittle rocks containing pre-existing flaws under uniaxial compression." *Engineering Fracture Mechanics*, 69(17), pp. 1853–1871. 2002. [10.1016/S0013-7944\(02\)00065-6](https://doi.org/10.1016/S0013-7944(02)00065-6)
- [35] Wong, R. H. C., Chau, K. T. "Crack coalescence in a rock-like material containing two cracks." *International Journal of Rock Mechanics and Mining Sciences*, 35(2), pp. 147–164. 1998. [10.1016/S0148-9062\(97\)00303-3](https://doi.org/10.1016/S0148-9062(97)00303-3)